Nuclear Engineering and Design 238 (2008) 3542–3550

Contents lists available at ScienceDirect

Nuclear Engineering and Design

journal homepage: www.elsevier.com/locate/nucengdes

PARIS project: Radiolytic oxidation of molecular iodine in containment during a nuclear reactor severe accident
Part 1. Formation and destruction of air radiolysis products—Experimental results and modelling

L. Bosland[a,*], F. Funke[b], N. Girault[a], G. Langrock[b]

[a] Institut de Radioprotection et de Sûreté Nucléaire, DPAM, SEMIC, LETR - CEN Cadarache, BP 3, 13115 Saint Paul Lez Durance, France
[b] AREVA NP GmbH, Technical Center, P.O. Box 1109, D-91001 Erlangen, Germany

ARTICLE INFO

Article history:
Received 4 December 2007
Received in revised form 20 June 2008
Accepted 29 June 2008

ABSTRACT

In case of a hypothetical severe accident in a nuclear LWR (light water reactor), the high radiation fields reached in the reactor containment building due to the release of fission products from the reactor core could induce air radiolysis. The air radiolysis products could, in turn, oxidise gaseous molecular iodine into aerosol–borne iodine–oxygen–nitrogen compounds. Thereby, this reaction involves a change of iodine speciation and a decrease of iodine volatility in the reactor containment atmosphere. Kinetic data were produced within the PARIS project on the air radiolysis products formation and destruction, and on their reaction with molecular iodine, with the objective of developing and validating existing kinetic models.

The current paper includes the non-iodine tests of the PARIS project whose objective was to determine the rates of formation and destruction of air radiolysis products in the presence of both structural containment surfaces (decontamination coating ("paint") and stainless steel), aerosol particles such as silver rich particles (issued from the control rods) in boundary conditions representative for LWR or PHEBUS facility containments.

It is found that the air radiolysis products concentration increases with dose and tend to approach saturation levels at doses higher than about 1 kGy. This behaviour is more evident in oxygen/steam atmospheres, producing ozone, than in air/30% (v/v) steam atmospheres, the latter favouring the model-predicted ongoing production of nitrogen dioxide even at very high doses. No significant effect of temperature, dose rate and hydrogen addition (4%, v/v) was observed. Furthermore, the inserted surfaces do not exhibit significant effects on the air radiolysis concentrations. However, these "non-noticeable influence" could be due to a masking of small effects by the appreciable scattering of the experimental air radiolysis product concentrations.

The PARIS results are then analysed using two different kinetic models, an empirical and a mechanistic one. The kinetic constants within an empirical model including formation and destruction of air radiolysis products, derived from PARIS results, are in reasonable agreement with those determined previously for lower steam fractions.

From the mechanistic model IODAIR-IRSN, it is concluded that ozone is the predominant air radiolysis product at low doses in air/steam atmospheres. At doses higher than 1 kGy, nitrogen dioxide becomes increasingly important, both due to an increase in its concentration and due to a simultaneous decrease in ozone concentration.

1. Introduction

In case of a hypothetical severe accident in a nuclear light water reactor (LWR), a large amount of radioactive fission product iodine may be released from the reactor core into the reactor containment, from where it represents a major radiological hazard to the environment. Knowledge of the behaviour of the iodine in such conditions is therefore necessary to study the impact of iodine mitigation measures to prevent or minimise iodine release to the environment.

The iodine inventory in the containment atmosphere depends on numerous physico-chemical processes such as deposition at and

* Corresponding author.
E-mail address: loic.bosland@irsn.fr (L. Bosland).

0029-5493/$ – see front matter © 2008 Elsevier B.V. All rights reserved.
doi:10.1016/j.nucengdes.2008.06.023

resuspension from surfaces, reactions in sumps and in containment atmosphere, and iodine exchange between sump and atmosphere. Furthermore, iodine speciation and thus iodine volatility is influenced by these processes.

An important chemical process in the atmosphere is, due to the high radiation field, the radiolytical oxidation of gaseous molecular iodine forming iodine oxides (IO_x). This means that a volatile gaseous iodine species is converted into an aerosol–borne iodine species, which means that the gas–borne iodine depletion rate by deposition could be changed. Previous experiments revealed that the destruction of molecular iodine (I_2) can be explained as a reaction of I_2 with air radiolysis products (ARP) (Funke et al., 1999). ARP (ozone included) and many further shorter-lived products (radicals such as N°, e^-, O°, OH°, etc.) from the radiolysis of the air/steam containment atmosphere, are formed and destroyed in the high radiation field. An empirical model was derived (Funke et al., 1999), integrating earlier Canadian work on the reaction between I_2 and ozone (O_3) (Vikis and MacFarlane, 1985). The resulting model predicts a very fast conversion of I_2 into IO_x in containment conditions, and that iodine gas phase speciation is dominated by iodine oxides rather than I_2. However, the underlying database was built only at comparatively high I_2 concentrations, and the effect of surfaces for iodine deposition and for ARP destruction were ignored in the experiments. Consequently, implementation of this empirical model on radiolytic oxidation into severe accident iodine codes would have been premature. The development of mechanistic models on radiolytic iodine oxidation (Narayanan, 2000; Dickinson and Sims, 2000; Aubert, 2002) also suffers from a lack of experimental data.

The Program on Air Radiolysis and Iodine adsorption on Surfaces (PARIS) was therefore initiated in 2002 by IRSN (Institut de Radioprotection et de Surêté Nucléaire), as part of the research programs performed by this Institute to improve severe accident modelling and evaluation of subsequent fission product release into the environment. This program was furthermore performed in collaboration with AREVA NP (formerly Framatome ANP) with the objective of measuring:

- the rate and amount of ARP production and destruction,
- rate and extent of radiolytic oxidation of molecular iodine into iodine oxides,
- the effect of the containment structural surfaces, namely decontamination coating ("paint") and stainless steel, on radiolytic oxidation of I_2,
- the effect of silver, representing silver-containing aerosol particles, on radiolytic oxidation of I_2.

Important new features of the PARIS project (as compared to the previous work) were: (1) more realistic low iodine concentrations, (2) surface to volume ratios of paint, steel and silver surface area to containment volume ratio representative of LWR or PHEBUS (Clément et al., 2003; Girault et al., 2006) facility containments, (3) higher steam fractions and (4) representative dose rates. The PARIS database was intended to provide data to develop and validate empirical models, and finally to derive a simplified model for ASTEC (Accident Source Term Evaluation Code) (Van Dorsselaere, 2005) and other severe accident iodine codes.

The PARIS database includes about 400 tests, about half of them without iodine. These tests whose objective was to measure the kinetics of air radiolysis products formation and destruction in the presence of surfaces, will be presented in the current paper, together with the interpretation of results. The test series involving iodine will be presented and interpreted in the forthcoming second part of this paper.

2. Experimental

The objectives of the experiments were to determine the kinetics of ARP formation and destruction kinetics and to quantify the effect of surfaces (stainless steel AISI 316 L, RIPOLIN paints and metallic silver) on air radiolysis product concentrations within boundary conditions (atmospheric composition, temperature, dose rate, areas of surfaces) representative to LWR containments and PHEBUS facility containments.

The general experimental procedure was to establish the desired composition of gases in 1-L glass flasks, optionally to add surface coupons, to irradiate the glass flasks at given dose rates until the desired doses were reached, and to subsequently determine the final air radiolysis products concentrations by an off-line method.

2.1. Filling of irradiation flasks

For cleaning, the glass flasks (Duran® borosilicate glass) were washed with acetone and water and heated up to 500 °C at least for 6 h in order to remove all potential organic impurities.

The volume of the glass flasks is 1.12E−3 m^3, and the inner surface area is 6.8E−2 m^2. Thus, the surface area/volume ratio is 60.7 m^{-1}.

In own previous experiments it was observed that injected ozone is not significantly destroyed by Duran glass surface (only 15% decrease during 3 days contact time at 20 °C). More stable ARP as e.g. NO_2 or N_2O should show an even higher stability towards glass.

The experimental apparatus for filling the flasks is shown in Fig. 1. The glass flasks were heated up to the temperature of the subsequent irradiation and evacuated. Optionally, 4% (v/v) hydrogen could be added. Pressure equilibration with the ambient pressure was then obtained by introducing mixtures of air/30% (v/v) steam or oxygen/30% (v/v) steam mixtures. The air/steam or oxygen/steam mixtures were obtained by passing air or oxygen through a thermostated water bath (Milli-Q quality). Synthetic air (<0.1 ppm hydrocarbon (C_nH_m, NO_x) and <0.5 ppm H_2O) or oxygen (purity > 99.999%; <0.2 ppm hydrocarbon (C_nH_m), <3 ppm H_2O and <0.2 ppm C_nH_m and CO_2) were provided by Linde or Air Liquide. When investigating the effect of surface samples, they were introduced in the "batch" reactor before evacuating and filling with gases.

2.2. Irradiations

Irradiations were performed at the Co-60 source of the Technische Universität München at Garching (Heusinger and Gruhn, 1970). Typically, dose rates of 0.3 and 1 kGy/h were applied at temperatures of 80 or 130 °C. Doses between 0.05 and 100 kGy were achieved. Heating was performed by immersion into heating baths. The temperature of the bath was kept constant throughout the irradiation with a heating plate regulated to provide a constant for temperature with a variation of less than ±5 °C. After the irradiation, any coupons were recovered prior to the analyses of the air radiolysis products.

2.3. Experimental determination of ARP concentrations

The so-called KI method, originally developed to measure ozone (O_3) concentrations (VDI, 1978), was chosen to determine ARP concentrations (Langrock and Funke, 2005). It consists of washing the whole content of a flask with an aqueous KI (potassium iodide) solution of about 5 ml with 20 g KI/L, pH 6.8, phosphate-buffered. During this procedure, ARP such as O_3 oxidise aqueous iodide into

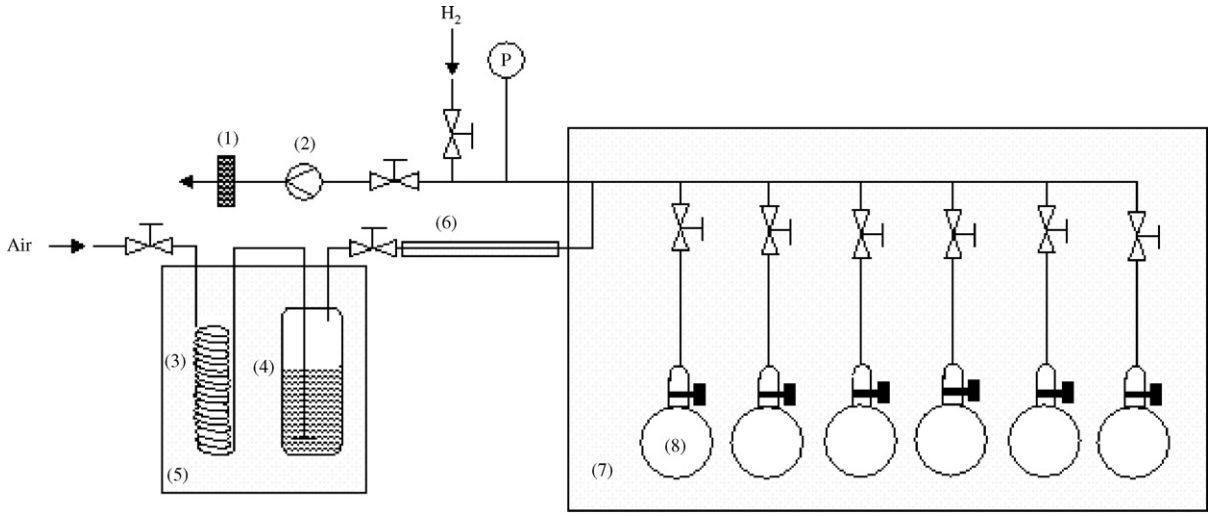

Fig. 1. Filling of glass flasks before irradiation in PARIS tests. Up to six glass flasks are filled in one step. (1) Charcoal filter, (2) vacuum pump, (3) heat exchanger, (4) humidifier/I_2-dosing, (5) thermostat, (6) heated tube, (7) hot-air cabinet, and (8) irradiation flask.

tri-iodide (I_3^-) according to:

$$O_3 + 2KI + H_2O \Rightarrow I_2 + O_2 + 2KOH$$

$$I_2 + I^- \Leftrightarrow I_3^-$$

The I_3^- concentration is sensitively measured by UV/vis at 350 nm, the detection limit for ARP in the gas phase is about 1×10^{-9} mol/L.

The KI method can be used due to the strong oxidation potential of ozone in aqueous solutions ($E^0(O_3/O_2) = 2.076$ V in acidic ($a_{H^+} = 1$) and $E^0(O_3/O_2) = 1.24$ V in basic ($a_{OH^-} = 1$)) solutions to convert iodide into molecular iodine ($E^0(I^-/I_2) = -0.536$ V) (Lide and Frederikse, 1995/1996). It should be noted that in principle also other wet procedures could be used for measuring ozone and other ARP, but the KI method was chosen due to its lower detection limit.

It is important to keep in mind that the iodide solution is used only as an indicator for ozone. No statement about the oxidation potential of ozone against I_2 in the gas phase is concluded from these measurements in aqueous phase. The reaction of ozone and other ARP with gaseous I_2 was investigated in the second part of the PARIS project to be published in a separate article. In the aqueous phase, reactions of ozone and other air radiolysis products with the I_2 intermediately formed are unlikely due to the huge excess of iodide over I_2.

Other relatively stable air radiolysis products besides O_3 should, in theory, oxidise KI, based upon comparison of oxidation potentials of I^-/I_2 with those of O_3/O_2, NO/N_2O ($E^0 = 1.591$ V ($a_{H^+} = 1$), $E^0 = 0.76$ V ($a_{OH^-} = 1$)), NO_2/NO ($E^0(N_2O_4/NO) = 1.035$ V)), N_2O/N_2 ($E^0 = 1.766$ V), and HNO_3/HNO_2 ($E^0 = 0.934$ V). However, it was found in separate tests that the KI method is not sensitive to N_2O and HNO_3, but sensitive to NO_2. In a separate test, two glass flasks were filled with synthetic air and steam at 80 °C. One flask was additionally filled with 5.1E−6 mol/L NO_2, the second flask with 6.8E−6 mol/L N_2O. After 1 h and in the absence of radiation, KI solution was injected into the flasks and the resulting "ozone" concentration was measured. In the NO_2 flask an "ozone" concentration of 9.5E−7 mol/L was found, whereas in the N_2O flasks only 3.9E−9 mol/L "ozone" was found, which is near the detection limit. Furthermore, the later on discussed mechanistic air radiolysis code IODAIR-IRSN shows that NO is clearly less important than NO_2 in the conditions of the PARIS tests.

2.4. Surface samples

O_3 is known to be destroyed at metallic surfaces by oxidising the surface (Thomas et al., 1997; Zakharov et al., 2001). The same is expected to hold for many other ARP. This effect has an important impact on severe accident iodine chemistry, because less ARP are then available for the radiolytic oxidation of molecular iodine in the containment atmosphere. In the PARIS tests simulating the appropriate boundary conditions, involving iodine, the decrease of molecular iodine should be affected by the presence of surfaces destroying the ARP. Radiolytic oxidation of I_2 should be slowed down with increasing surface area to volume ratios. Of course, I_2 is also reduced in parallel due to deposition at these surfaces.

The surface types and surface areas studied in the PARIS program (stainless steel, epoxy paint and silver) were therefore defined to be representative of LWR and PHEBUS facility containments. The geometric characteristics of the experimental surface samples are shown in Table 1.

The chemical composition of stainless steel coupons (AISI 316 L) is indicated in Table 2. They contain 2 wt% Mo which should provide greater protection against pitting and thus also should weaken their corrosion by halogens, and in particular iodine.

The epoxy paint coupons mostly contain a polymer (an alcohol polyamine in our case) and a hardener (consisting of an epoxy liquid from a bisphenol (60%) plus a cycloaliphatic polyamine (30%)). Pigments (such as SiO_2 and TiO_2) are also contained in the paint.

Silver was provided by Johnson Matthey (purity > 99.9%) in the form of foils. Before experiments, the silver surface was washed with water and acetone and then heated for cleaning. It had a shiny appearance, thus guaranteeing the absence of any important oxide layer on the surface stemming, e.g. from storage at ambient conditions.

2.5. Quality of data

A total of 215 irradiation tests were performed in the PARIS project on ARP production and destruction, blind tests and repeating test included. As was often observed in previous irradiated work (e.g. Funke et al., 1999), scattering of data was also observed in the PARIS tests. Partly, averaging of ARP concentrations measured at equal doses and with the same boundary conditions was performed. Nevertheless, the below discussed ARP concentrations still

Table 1
Geometric dimensions of the different coupons

	Substrate			
	Stainless steel	Epoxy paint		Silver
Length (cm) × width (cm) × height (cm)	0.8 × 0.8 × 0.5	1.3 × 1.0 × 0.5	0.9 × 0.9 × 0.5	14.9 × 0.75 × 0.025
Surface area (cm^2)	2.88	4.9	3.4	23.1
Objective S/V (cm^{-1}) LWR/PHEBUS FP	0.003	0.005	0.0035	0.02 (LWR)
Ratio surface coupon/glass surface	0.004	0.007	0.005	0.034

V is the gaseous volume, S is the coupon surface area. LWR means approximate values for a typical LWR containment.

Table 2
Chemical composition of the 316-L stainless steel coupons

Element	Weight fraction (%)
Ni	10.5–13
Cr	16–18
Fe	Balance
C	<0.03
Mn	<2
S	0.03
Si	0.75–1
P	0.04
Co	0.2
Mo	2–2.4

show pronounced scatterings, providing an insight into the uncertainties associated to the individual data points in these plots.

3. Models description

Two different model approaches were used in order to analyse the experimental results, a mechanistic model allowing to study detailed reaction mechanisms (IODAIR-IRSN) (Aubert, 2002), and an empirical model suitable for inclusion into severe accident containment codes.

3.1. Mechanistic model

The mechanistic model IODAIR as developed by IRSN (Aubert, 2002) represents a recent improvement of earlier Canadian model development (Narayanan, 2000). It is mainly based on data from mass spectroscopy and electron impact studies (Willis et al., 1970; Willis and Boyd, 1976). Excitation and ionisation mechanisms for the production of primary air radiolysis products as well as their interaction kinetics are taken into account. Around 200 chemical reactions are included by coupled differential equations to treat the reaction kinetics.

The production rate of the primary species "i" during irradiation is given by

$$\frac{dX_i}{dt} = G_i \frac{dD}{dt} \frac{1}{N} \times 100 \quad (1)$$

X_i represents the concentration of species i (mol/L). G_i represents the number of molecules i produced (in case of positive G) per 100 eV or destroyed per 100 eV (in case of negative G) absorbed by the irradiated medium ($1G$ corresponds to 1.0364×10^{-7} mol J^{-1}). The G_i values corresponding to the formation of primary products from radiolysis of pure oxygen, nitrogen, hydrogen and water, respectively, are shown in Fig. 2 (Willis et al., 1970; Willis and Boyd, 1976; Armstrong and Willis, 1976; Aubert, 2002). D is the dose (eV L^{-1}) and N is Avogadro's number (mol^{-1}).

The primary species can react with each other and with the initial molecules through several reactions producing secondary species that may or may not take part in further reactions. Moist air, which represents a complex medium during irradiation, leads to effective G values that depend on both the irradiation conditions (mainly the radiation energy) and the O_2, N_2 and H_2O mass fractions.

3.2. Empirical model

The empirical kinetic model simply treats two processes, the formation and the destruction of air radiolysis products (Funke et al., 1999):

$$\frac{d[ARP]}{dt} = k_1 D - k_3 [ARP] D \quad (2)$$

with

- [ARP]: concentration of ARP (mol/L),
- k_1: rate constant of ARP formation by air radiolysis (mol L^{-1} s^{-1} $(kGy/h)^{-1}$),
- k_3: rate constant of ARP decomposition during irradiation (s^{-1} $(kGy/h)^{-1}$),
- D: dose rate (kGy/h^{-1}).

The model is based upon previous irradiation tests performed in air and air/steam mixtures between 20 and 130 °C and dose rates of about 1.5–2 kGy/h (Funke et al., 1999). It is worthwhile to note that the same analytical procedure (KI method) as in the PARIS tests was applied to determine the ARP concentrations. However, the steam fractions were generally lower than in the PARIS tests.

This empirical model treats the ARP production as a zero-order process whereas ARP destruction follows a first-order kinetics law. Consequently, decomposition of ARP is accelerated during build up of ARP concentration, and an equilibrium concentration is achieved at sufficiently high doses, where $k_1 = k_3$ [ARP]. Values of rate constants taken from Funke et al. (1999) are given in Table 4.

As described above, surfaces lead to the depletion of ARP concentration. As this depletion requires in a first step the deposition of the ARP at the surface, it is reasonable to tentatively add a pseudo-first-order kinetic disappearance term, as often used in severe accident iodine surface models (Funke et al., 1996; Wren et al., 1999), to Eq. (2):

$$\frac{d[ARP]}{dt} = k_1 D - k_3 [ARP] D - k_D \frac{S}{V} [ARP] \quad (3)$$

with

- S: surface area of the coupon introduced in the vessel (m^2),
- V: volume of the vessel (m^3),
- k_D: ARP destruction constant due to the impact of the surface ($m.s^{-1}$).

The rate constant k_D generally depends on temperature and on surface type (paint, steel, silver).

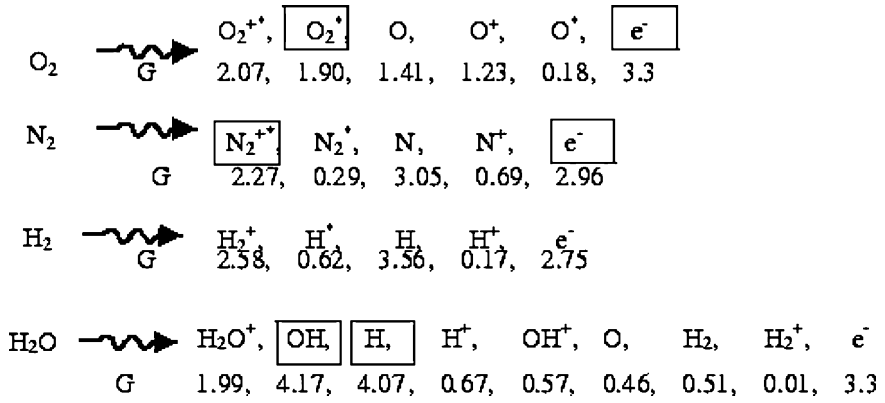

Fig. 2. G value (1.0364×10^7 mol J^{-1}) of the primary products formation from radiolysis of pure oxygen, nitrogen and water.

4. ARP formation and destruction in the absence of surface coupons

4.1. Analyses with the empirical model

The rate constants of the empirical model were fitted in this work without taking into account previous values for the rate constants k_1 and k_3 and their respective activation energies as given in Funke et al. (1999). Instead, optimisations of k_1 and k_3 were realized with the use of the FACSIMILE software (FACSIMILE, 2008). The best agreement between the experimental and calculated values is obtained at the minimum of the standard deviation.

The empirical model was applied in this work using initial ARP concentrations of 10^{-9} mol/L according to natural ozone concentrations in ambient air as measured by the KI method in unirradiated tests.

4.1.1. Base case: 80 °C, air/steam/hydrogen

Experimental data obtained in an air/steam/H_2 atmosphere at 80 °C are arbitrarily defined as a base case. Fig. 3 shows the evolution of measured ARP concentrations as function of the dose. Despite the noticeable scatter of the experimental ARP concentrations (factors 5–10), an increase of the ARP concentration with the dose is clearly evidenced. According to the empirical model, the rate constant for the ARP production is $k_1 = 4.8 \times 10^{-11}$ mol L^{-1} s^{-1} (kGy/h)$^{-1}$, and the rate constant for ARP destruction is $k_3 = 2.4 \times 10^{-5}$ s^{-1} (kGy/h)$^{-1}$. ARP formation is predominant at low doses ($D < 1$ kGy), whereas ARP destruction gains in importance for doses greater than 10 kGy. The model formally leads to a plateau in the ARP concentration at high doses of about 30–40 kGy. However, this is neither supported by nor in conflict with the experimental data. It should be noted that only two data points were measured at very high doses (near 100 kGy), and this clearly reduces the accuracy of the fitted k_3 value. The model is obviously not in conflict with the data, but the determination of an ARP destruction rate from these data alone remains uncertain, even there is no proof of the establishment of an equilibrium ARP concentration.

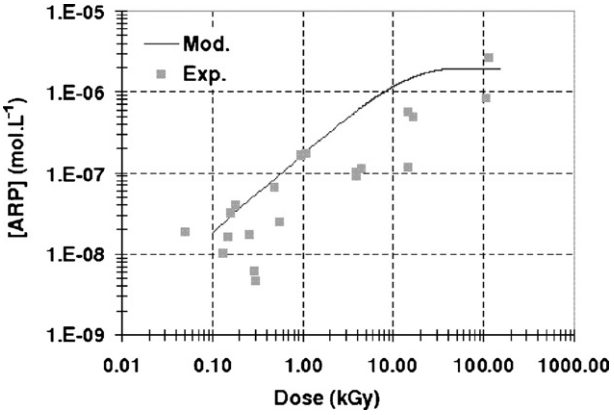

Fig. 3. ARP concentrations as function of the dose at 80 °C in an air/30% (v/v) steam/4% (v/v) H_2 atmosphere and optimised empirical model.

4.1.2. Parameter effects

The impact of various parameters such as dose rate, temperature and atmospheric composition, on the rates of ARP formation and destruction was studied by fitting individual values of k_1 and k_3 under the respective boundary conditions.

The dose rate was varied experimentally between about 0.3 and about 1 kGy/h. As expected from the previous project (Funke et al., 1999), ARP concentrations are a function of dose as the product of dose rate and irradiation time. At least within this limited range of dose rates, it is allowed to consider the dose rate just as a parameter to calculate the dose.

Table 3 summarizes the optimized rate constants of ARP formation and destruction using the empirical model in the various atmospheres and the two temperatures.

There is no consistent trend regarding the values for k_1 and k_3 with temperature. Instead, considering the experimental uncertainties and the associated anticipated model parameter uncertainties, the rate constants k_1 and k_3 are independent of temperature in all three different atmospheric mixtures. In

Table 3
Rate constants of ARP formation and destruction from analyses of PARIS data for various atmospheres at 80 °C and at 130 °C

	ARP formation constant, k_1 ($\times 10^{11}$ (mol L^{-1} s^{-1} (kGy/h)$^{-1}$)		ARP destruction constant, k_3 ($\times 10^4$ s^{-1} (kGy/h)$^{-1}$)	
	80 °C	130 °C	80 °C	130 °C
O_2/steam	1.2	2.7	1.0	1.6
Air/steam	2.4	2.6	1.0	0.6
Air/steam/H_2	4.8	2.1	0.2	0.1

Table 4
Rate constants of ARP formation and destruction in an air/steam mixture for various temperatures from previous project (Funke et al., 1999)

Temperature (°C)	k_1 ($\times 10^{11}$ mol L^{-1} s^{-1} (kGy/h)$^{-1}$)	k_3 ($\times 10^{4}$ s^{-1} (kGy/h)$^{-1}$)
20	7.0 ± 1.0	0.3 ± 0.1
80	5.4 ± 0.7	2.4 ± 0.4
130	4.4 ± 0.6	7.6 ± 1.4

the case of ARP destruction, this temperature independency is not consistent with previous data from Funke et al. (1999) as shown in Table 4, where k_3 increases with temperature. However, the above-mentioned data scattering and the associated uncertainty of the k_3 determination could hide such a temperature effect.

Hydrogen, according to Table 3 data at 80 °C, seems at first sight to exhibit an increasing effect on ARP formation and a decreasing effect on ARP destruction. However, such an effect is not supported by the 130 °C results. Moreover, any effect suggested by the 80 °C data could be due to the uncertainties of the experimental data. It is also noted that the PARIS data in air/steam/hydrogen lead to an ARP formation rate constant which is fully consistent with the equivalent rate constant from previous data in hydrogen-free air/steam atmosphere (Table 4). In this latter case, no conclusion from limited ARP destruction rate differences as function of hydrogen presence should be drawn because of the above-mentioned general uncertainty of k_3 determination in the PARIS database. To conclude, no significant effect of a 4% (v/v) hydrogen component in the air/steam mixture is deduced. There might be a small effect, but this cannot be quantified using the available database.

Replacing the air by pure oxygen offers the possibility to experimentally exclude nitrogen compounds from the reaction mixture, and to study formation and destruction of ozone alone, without the NO_2 component.

In oxygen/steam atmospheres the ozone concentration reaches saturation at doses greater than about 1 kGy at 130 °C as shown in Fig. 4. Analogous to the above discussed of ARP equilibrium concentration, this is explained by equilibrium between formation and destruction of ozone. From the determined kinetics rate constants and taking into account their associated uncertainties, no clear effect of removing nitrogen from the reaction system on ARP formation/destruction can be deduced. However, comparing the saturation levels in Figs. 3 and 4, the modelled ARP equilibrium concentration in oxygen/steam is higher by a factor of 10 as compared to the steam/air condition. Nevertheless, this difference could

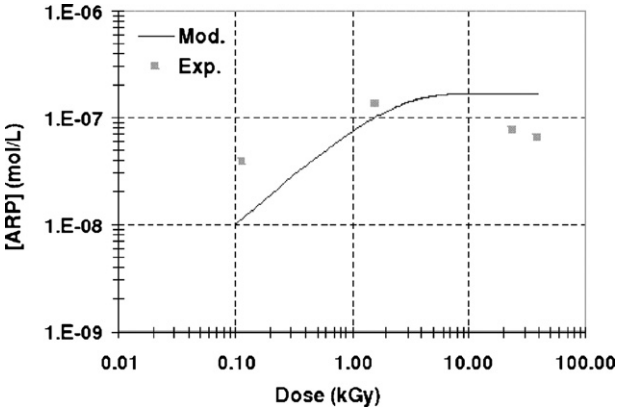

Fig. 4. Evolution of O_3 concentration versus dose at 130 °C in an oxygen/30% (v/v) steam atmosphere, comparison of data and empirical model.

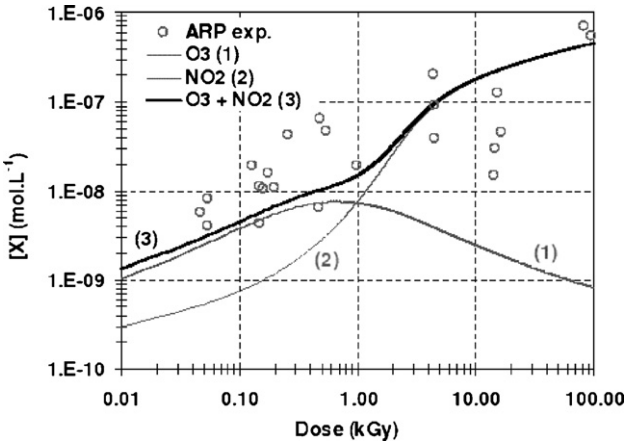

Fig. 5. Experimental ARP concentrations and calculated concentrations of O_3, NO_2 and their sum from IODAIR-IRSN at 80 °C in air/steam atmosphere.

also be explained to be the result of experimental uncertainties in k_3 determinations.

4.2. Study with IODAIR-IRSN model

In contrast to the empirical model, the mechanistic IODAIR-IRSN model allows to analyse the evolution of the individual ARP. As noted earlier, only ozone and nitrogen dioxide are supposed to be detected experimentally by the KI method, but not HNO_3 or N_2O. Therefore, the following IODAIR results only deal with O_3 and NO_2.

The starting O_3 concentration in the IODAIR calculations was always of 10^{-9} mol/L, consistent with the analyses using the empirical model.

4.2.1. Base case: 80 °C, air/steam

Fig. 5 shows the evolution of O_3 and NO_2 concentrations, and of their sum at 80 °C in an air/steam (30% v/v) mixture as calculated by IODAIR and compares these with the experimental data. A relatively good agreement between the ARP concentration measured by the KI method and the sum of calculated O_3 and NO_2 concentrations is observed. There appears to be a slight underestimation of the experimental ARP concentrations for doses lower than 1 kGy which is not explained yet. Moreover, the model suggests that O_3 is the predominant ARP species only at doses lower than 1 kGy, and that NO_2 is the predominant air radiolysis product above 1 kGy.

The analogous analysis of the experimental data in air/steam at 130 °C confirms the trends of the above 80 °C results (Fig. 6).

4.2.2. Influence of the hydrogen

Fig. 7 shows that the model results at 80 °C in air/steam/hydrogen mixture are generally in good agreement with the experimental data.

Considering only the experimental results in Figs. 5 and 7, no clear experimental influence of hydrogen on ARP concentrations would be concluded. However, the IODAIR-IRSN results themselves predict that:

- addition of hydrogen decreases the O_3 concentration over the whole range of studied doses.
- at intermediate doses 0.1 kGy < D < 1 kGy, NO_2 is increased by about one order of magnitude in presence of hydrogen,
- at higher doses, similar NO_2 concentrations are reached in both atmospheres, with and without hydrogen.

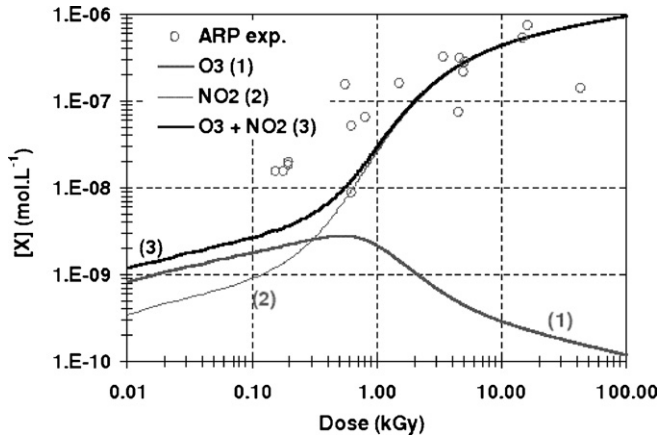

Fig. 6. Experimental ARP concentrations and calculated concentrations of O_3, NO_2 and their sum from IODAIR-IRSN at 130 °C in air/steam atmosphere.

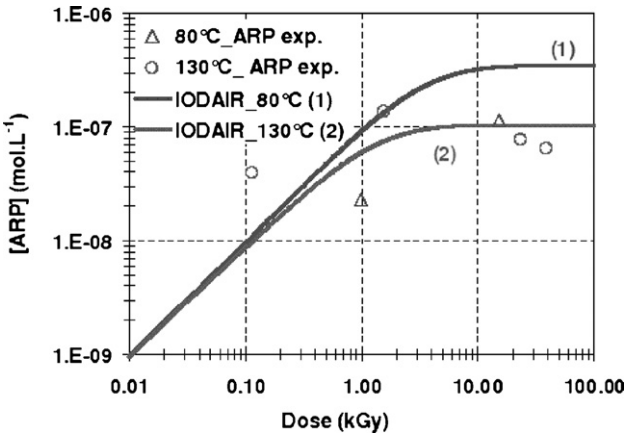

Fig. 8. Experimental ozone concentrations and ozone concentrations calculated with IODAIR-IRSN at 80 and 130 °C in an oxygen/steam atmosphere.

Therefore, hydrogen seems to strengthen NO_2 formation at the expense of O_3, especially at medium and high doses. Consequently, according to IODAIR results in Fig. 7, NO_2 is dominant over O_3 already at doses above 0.1 kGy.

4.2.3. Results in oxygen/steam atmosphere (influence of nitrogen removal)

Fig. 8 shows experimental and calculated ozone concentrations in oxygen/steam mixtures at 80 and 130 °C. At about 10 kGy, the O_3 concentration reaches a saturation level, similar to the prediction of the empirical model. The calculated equilibrium O_3 concentrations are also similar to those of the empirical model.

Thus, the mechanistic model confirms in some way the empirical model concerning equilibrium between O_3 formation and O_3 destruction, as long as no nitrogen is included in the atmosphere. In air/steam atmosphere including nitrogen, the additional and long-term NO_2 formation even at very high doses effectively retards the establishment of equilibrium between ARP formation and destruction.

4.2.4. Influence of the temperature

No influence of temperature on the ARP concentration was concluded from PARIS data at 80 and at 130 °C in air/steam, air/steam/hydrogen and oxygen/steam atmospheres. At least for the air/steam atmosphere, this seems to be in conflict with previous data (Funke et al., 1999). However, as stated already earlier, the data scattering could have masked such a temperature effect in the PARIS tests.

IODAIR-IRSN calculations in oxygen/steam atmosphere predict that the stability of ozone is decreasing with increasing temperature (Fig. 8). This would be consistent with previous data in air and air/steam from Funke et al. (1999), but the few scattering PARIS data are not suitable to confirm such a temperature dependency. Therefore, PARIS data are not expected to confirm or improve current approaches for the temperature dependencies.

5. ARP formation and destruction in the presence of surface coupons

Ozone is destroyed upon contact with various surfaces (Thomas et al., 1997; Zakharov et al., 2001). In order to study the destruction of ozone and ARP in general at surfaces, various surface coupons (stainless steel, epoxy paint and silver) were introduced into the irradiated test flasks for irradiation. Both, the empirical and the mechanistic model were used to optimise the destruction rate constant in Eq. (3), which was also implemented into the mechanistic IODAIR-IRSN code. The effect of silver on ozone concentrations in oxygen/steam atmosphere at 80 °C is shown in Fig. 9, where experimental ozone concentrations are lowered by roughly one order of magnitude in the presence of silver. Fig. 9 also displays the results

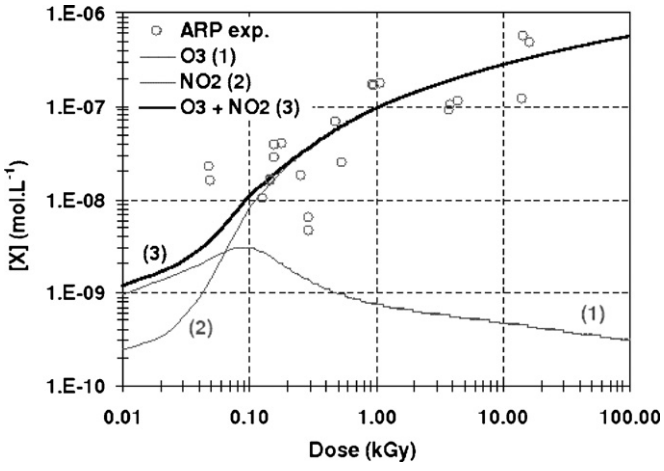

Fig. 7. Experimental ARP concentrations and calculated concentrations of O_3, NO_2 and their sum from IODAIR-IRSN at 80 °C in air/steam/hydrogen atmosphere.

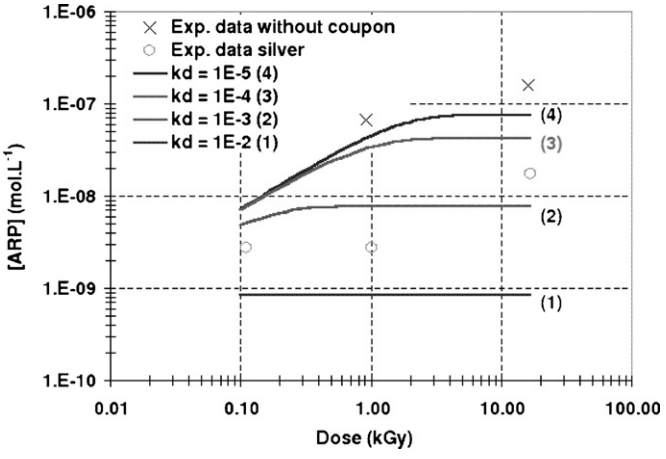

Fig. 9. Experimental ozone concentrations and ozone concentrations calculated with the empirical model in oxygen/30% (v/v) steam atmosphere at 80 °C with or without silver coupon (22 cm^2).

Table 5
Effect of surfaces on ARP or ozone build-up

Temperature (°C)	Nature of the coupon	Effect on ARP or ozone build-up O_2/steam atmosphere	Effect on ARP or ozone build-up air/steam atmosphere
80	Stainless steel (3 cm^2)	Not conclusive	Not conclusive
	Painted stainless steel (4 cm^2)	Not conclusive	Not conclusive
	Silver (22 cm^2)	1E−3 m/s	Not conclusive
130	Stainless steel (3 cm^2)	Not conclusive	Not conclusive
	Painted stainless steel (4 cm^2)	Not conclusive	Not conclusive
	Silver (22 cm^2)	Not conclusive	Not conclusive

of the empirical model, applied by varying ozone destruction rates. The optimum ozone destruction rate k_D in this particular boundary condition is close to 1E−3 m/s. A more accurate determination of this rate constant is not possible, given the large scattering of data and the small set of data. Fig. 10 provides the same data as in Fig. 9, but this time compared to calculations with the mechanistic IODAIR model. The same conclusion on the ozone destruction rate close to 1E−3 m/s is drawn, which means that the derived effect of surfaces on the ozone concentration is not depending on the type of the calculation model.

In contrast to the above 80 °C data, an effect of silver on ozone concentration at 130 °C in oxygen/steam is not identified. The same conclusions are drawn from analyses of data obtained in air/steam and air/steam/hydrogen atmospheres at both temperatures, 80 and 130 °C, and for both, stainless steel and epoxy paint (Table 5). Fig. 11 provides a typical result. Generally, scattering of data and too few data points do not allow to identify any significant surface effects on ozone or ARP concentrations. All this favours the conclusion that even the above effect of silver at 80 °C in oxygen/steam could be an artefact.

For stainless steel and paints, these rather unexpected results could not be explained by too low surface-to-volume ratios as they are representative of typical LWR and PHEBUS FP containments.

However, if the glass surface would be really involved in ARP destruction, the effect of adding a small surface area of paint or stainless steel would be probably masked by the effect of the much larger surface area of the vessel walls.

For silver, it will be present as an aerosol in the containment atmosphere or finely deposited onto surfaces. Thus, in LWR reactors, the ratio of surface to volume could be higher or lower than used in the PARIS tests, depending on the aerosols size and specific surface. Obviously, modelling such an effect would require more precise silver/ARP data.

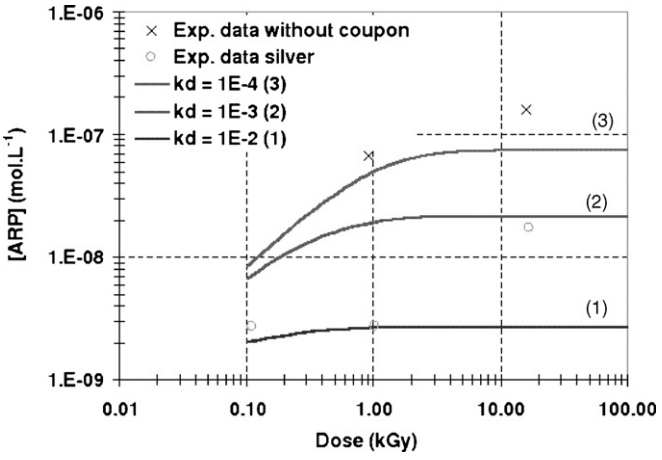

Fig. 10. Experimental ozone concentrations and ozone concentrations calculated with IODAIR-IRSN in oxygen/30% (v/v) steam atmosphere at 80 °C with or without silver coupon (22 cm^2).

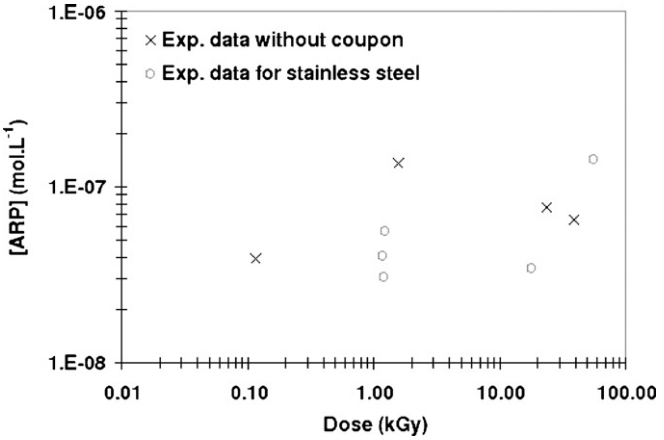

Fig. 11. Experimental ozone concentrations in oxygen/30% (v/v) steam atmosphere at 130 °C with or without stainless steel coupon (3 cm^2).

6. Conclusions

The PARIS project enlarges the experimental database on air radiolysis product formation and destruction in severe accident containment atmospheres with the performance of 215 tests on the production and destruction of air radiolysis products. From these tests, it was concluded that air radiolysis product concentrations increase with dose and that other quantities such as temperature, hydrogen up to 4% (v/v) and surfaces at representative surface/volume ratios do not show significant influences. It can, however, not be excluded that small effects could be hidden behind the appreciable scattering of data.

The increase of the air radiolysis product concentration with dose and the apparent approaching of a saturation level at least for oxygen/steam atmospheres support a simple empirical model, consisting of a zero-order production and a first-order destruction of air radiolysis products. Associated rate constants are derived from the PARIS data for all three atmosphere types, and these are roughly consistent with previous data on air radiolysis product build-up in irradiated tests in lower steam concentration regimes.

On the other side, high-dose data could also be interpreted as showing continuous increasing of air radiolysis product concentrations. Only in pure oxygen atmosphere, air radiolysis product clearly approaches a saturation level at doses higher than 1 kGy. In the frame of the mechanistic IODAIR-IRSN model on air radiolysis product formation, these findings are interpreted based upon the model prediction, that different spectra of air radiolysis products are produced in the different atmospheric compositions. From the mechanistic model, in air/steam atmospheres, ozone is a dominant species only at low doses, with a maximum at about 1 kGy. Contrarily, nitrogen dioxide becomes the dominant species at higher doses and does not achieve a saturation level within the studied experimental dose range of about 100 kGy. In oxygen atmosphere, ozone

is the dominant air radiolysis product and reaches a saturation level. The experimental determination of air radiolysis products is probably sensitive to the sum of both, ozone and nitrogen dioxide. Consequently, the experimental detection should find the saturation level in oxygen atmosphere, but not in air/steam atmospheres, as observed.

IODAIR-IRSN mechanistic code models well the ARP concentration that makes it suitable for the modelling of the ARP concentration in presence of radiation in conditions close to those of the PARIS project. Nevertheless, a simplified model is desirable for use in severe accident codes where reaction between air radiolysis products and gaseous iodine leads to radiolytic oxidation and formation of iodine oxides, i.e. I–O and I–O–N compounds with different stoichiometries. The empirical model, consisting of one production reaction and one destruction reaction for air radiolysis products, is in general able to describe the data. However, values of rate constants by fitting the model to PARIS data vary over large ranges when comparing with derived rate constants from a previous project (Funke et al., 1999). The analyses of the PARIS data allow to extend the existing models to much broader ranges of boundary conditions rather than providing new rate constants.

No noticeable effect of containment surfaces (typical of LWR and PHEBUS FP: epoxy paint, stainless steel, silver) is observed in the PARIS data. However, due to the strong scattering of data, no definitive conclusions on model rate constants of ARP or ozone destruction at surfaces can be formulated from the PARIS database.

It would be desirable in future experiments on air radiolysis product formation and destruction to measure ARP speciation, and to refine the concentration measurements. Higher doses should also be used to check where saturation levels in air/steam atmospheres are achieved. Even though primary, unstable air radiolysis products are known, also the unambiguous identification and quantitative determination of stable air radiolysis products to prove the validity of models describing the formation of ARP is required. As typical ARP concentrations are relatively low, very sensitive methods with low detection limits have to be used. Optical methods (e.g. Raman spectroscopy, flash photolysis) could provide useful information for the identification of ARP. For the support of those methods it could be useful to cool down an irradiated gas phase rapidly by thermal shock to freeze the composition of the gas phase or to liquefy the gas phase. Chromatographic techniques or mass-spectrometric techniques could also be suitable methods for the determination of chemically more stable compounds (e.g. N_2O, NO_2/N_2O_4). Such new data could also serve as a basis to simplify the mechanistic model.

The influence of silver aerosols on ARP formation and destruction was studied with a silver coupon in a first step. This should be developed in a second step with aerosols in order to highlight the uncertainties that remain in this field of study.

Acknowledgement

We thank F. Payot for his contribution to the preliminary interpretation of the results.

References

Armstrong, D.A., Willis, C., 1976. Excited states in the radiation chemistry of gaseous diatomic hydrides. International Journal for Radiation Chemistry 8, 212–235.
Aubert, F., 2002. Destruction par radiolyse gamma de l'iodure de methyl en faible concentration dans l'air humide. Thesis of the University Aix, Marseille III, France.
Clément, B., Hanniet-Girault, N., Repetto, G., Jacquemain, D., Jones, A.V., Kissane, M.P., Von der Hardt, P., 2003. LWR severe accident simulation: synthesis of the results and interpretation of the first PHEBUS FP experiment FPT0. Nuclear Engineering and Design 226, 5–82.
Dickinson, S., Sims, H.E., 2000. Development of INSPECT model for the prediction of iodine volatility from irradiated solutions. Nuclear Technology 129 (3), 374–386.
FACSIMILE, 2008. FACSIMILE, v4.0 User Guide. MCPA Software. http://www.mcpa-software.com.
Funke, F., Greger, G.U., Hellmann, S., Bleier, A., Morell, W., 1996. Iodine–Steel reactions under severe accident conditions in light-water reactors. Nuclear Engineering and Design 166, 357–365.
Funke, F., Zeh, P., Hellmann, S., 1999. Radiolytic oxidation of molecular iodine in the containment atmosphere. In: Proceedings of the OECD Workshop on Iodine Aspects of Severe Accident Management, Vantaa, Finland, May 18–20.
Girault, N., Dickinson, S., Funke, F., Auvinen, A., Herranz, L., Krausmann, E., 2006. Iodine behaviour under LWR accident conditions: lessons learnt from analyses of the first two PHEBUS FP tests. Nuclear Engineering and Design 236, 1293–1308.
Heusinger, H., Gruhn, B., 1970. Kerntechnik, Isotopentechnik und Chemie 12, 229–233.
Langrock, G., Funke, F., 2005. Synthesis of PARIS results (Program on Air Radiolysis, Iodine and Surfaces). Framatome ANP GmbH Report, NGTR/2005/en/0308.
Lide, D.R., Frederikse, H.P.R., 1995/1996. CRC Handbook of Chemistry and Physics, 76th edition. CRC Press.
Narayanan, A., 2000. A global model for iodine behaviour in containment, PhD University of Toronto, Canada.
Thomas, K., Hoggan, P.E., Mariey, L., Lamotte, J., Lavalley, J.C., 1997. Experimental and theoretical study of ozone adsorption on alumina. Catalysis Letters 46, 77–82.
VDI-Handbuch Reinhaltung der Luft, 1978. Messen der Ozon- und Peroxid-Konzentration. Manuelles photometrisches Verfahren, Kaliumiodid-Methode.
Van Dorsselaere, J.P., 2005. Development and assessment of ASTEC CODE for severe accident simulation. In: Proceedings of the 11th NURETH, Popes Palace Conference Center, Avignon, France, October 2–6.
Vikis, A.C., MacFarlane, R., 1985. Reaction of iodine with ozone in the gas phase. Journal of Physical Chemistry 89, 812–815.
Willis, C., Boyd, A.W., Young, M.J., 1970. Radiolysis of air and nitrogen–oxygen mixtures with intense electron pulses: determination of a mechanism by comparison of measured and computed yields. Canadian Journal Chemistry 48, 1515–1525.
Willis, C., Boyd, A.W., 1976. Excitation in the radiation chemistry of inorganic gases. International Journal for Radiation Physics and Chemistry 8, 71–111.
Wren, J.C., Glowa, G.A., Meritt, J., 1999. Corrosion of stainless steel by gaseous I_2. Journal of Nuclear Materials 265, 161–177.
Zakharov, I.I., Shapavalova, I.N., Zakharova, O.I., Tatarchenko, G.O., Tyupalo, N.F., 2001. A density functional study of ozone and oxygen surface structures on Ni(1 1 0). Journal of Structural Chemistry 42 (6), 888–893.